A theory for the viscous sublayer of a turbulent flow

By JOSEPH STERNBERG

Ballistic Research Laboratories, Aberdeen Proving Ground, Maryland

(Received 27 April 1961 and in revised form 12 September 1961)

The laminar sublayer and 'transition zone' are shown to be the region where the turbulent velocity fluctuations are directly dissipated by viscosity. A simplified linearized form of the equations of motion for the turbulent fluctuations is used to describe the turbulent field between the wall and the fully turbulent part of the flow. The mean flow in the viscous sublayer and the turbulent field outside the sublayer are assumed to be known from experiment. The thickness of the sublayer arises naturally in the theory and is directly analogous to the inner viscous region for the fluctuations in a laminar flow. It is shown that the large-scale fluctuations containing most of the turbulent energy are convected downstream with a velocity characteristic of the middle of the boundary layer. Thus Taylor's hypothesis does not apply to these large-scale fluctuations near the wall. The convective velocity found in the measurements of pressure fluctuations at the boundaries of turbulent flows is in accord with the theory. Calculations are given for the energy spectra and u' fluctuation level in the sublayer and other aspects of the fluctuation field are discussed. The linear pressure fluctuation field at the edge of the sublayer is calculated and found to be much larger than the nonlinear field. Examining the effect of strong free-stream turbulence on laminar boundary-layer transition, it appears that the physical model underlying Taylor's parameter is incorrect.

1. Introduction: the laminar sublayer

The laminar sublayer has been a subject of controversy and investigation for more than 20 years. The reason for this interest is that the nature of the flow close to the wall has an important influence on the heat, mass, and momentum transfer from the boundary. Furthermore, experiments have shown that the flow of energy from the mean flow to the turbulent motion is a maximum inside the sublayer. This fact suggests that an understanding of the structure of turbulence in a shear flow may depend on an understanding of the flow near the wall.

The original idea, Taylor (1916), was that in a turbulent flow there ought to be a thin fluid layer next to the surface free of turbulent motion, a true laminar layer. Studies of the stability of Couette flow (the flow between a fixed wall and a moving wall) had shown that there was a critical Reynolds number (≈ 300) below which all eddies would die out. The critical Reynolds number Uh/ν was formed using the velocity U of the moving wall and the separation distance h, where ν is the kinematic viscosity. It was postulated that the flow next to the wall was equivalent to a Couette flow. The laminar sublayer thickness δ_s could then be estimated by substituting δ_s for the separation distance in the stability analysis.

In 1932, Fage & Townend studied the fluctuation field close to the surface using an ultramicroscope for following minute particles in water. They found no evidence of an eddy-free region near the wall. An interesting discussion of this work is given by Taylor (1932) who examined the possible connexion between special types of disturbances where the velocity distributions were known and the turbulent fluctuation field found by Fage & Townend (1932). These experimental results were confirmed by later hot-wire measurements in air by Laufer (1950, 1953) and Kelbanoff (1954). Instead of being eddy free, the turbulence level, as given by the ratio of u' the root-mean-square value of the velocity fluctuation in the flow direction to the local mean velocity U_l reached a maximum value of approximately 0·4 close to the wall. Also the turbulent shear stress, as deduced from the mean-flow measurements, did not vanish in a thin region next to the wall, but instead varied continuously from zero at the wall to the level of the wall shear. Thus it has been clear for some time that a theory of the 'laminar' sublayer must account for the fact that the flow is turbulent all the way to the wall.

There is now a relative wealth of experimental information on the fluctuation field close to the wall of a turbulent flow. What is needed is a theoretical structure that will provide a rational foundation for the understanding and interpretation of the experimental observations. Several recent attempts have been made to develop phenomenological models for the flow in the sublayer. On the basis of some observations using dye in water, Einstein & Li (1956) were led to postulate the periodic growth and decay of a true laminar region near the wall. An equivalent model has been proposed by Hanratty (1956). However, in all these cases, agreement with the measurements of the mean and fluctuation field is sensitive to the choice of critical parameters as well as to arbitrary and sometimes inconsistent assumptions concerning the physical processes. The purpose of this paper is to make a start towards the development of a theory for the sublayer which follows from the Navier–Stokes equations without the need for phenomenological assumptions or tinkering with adjustable parameters.

We have already suggested that the sublayer is only a special part of the general turbulent fluctuation field in a bounded shear flow. The aim of the theory will be to describe as far as possible the direct influence of the wall on the fluctuation field. The turbulent field outside of this region of direct influence is assumed to be known on the basis of the experimental measurements. This knowledge is essential in the development of the sublayer analysis. Fortunately we need not be concerned with shear flow turbulence in all its complexity, since only certain fairly simple aspects of such flows are significant for this problem. However, some of the simple features have been obscured by the accepted methods for presenting the experimental results. It is customary to determine the space scales or wave-numbers for the turbulent measurements by using Taylor's hypothesis (Taylor 1938) to justify the necessary space-time transformation. Our first step will be to show that this hypothesis, which was introduced to represent the turbulence behind a grid in a wind tunnel, is not valid in a shear flow, especially near a wall. This analysis will provide a basis for re-interpreting the experimental measurements and will make possible some important simplifications in the subsequent development of the theory.

2. Taylor's hypothesis in a shear flow

Taylor's hypothesis, which has been amply verified for a uniform low-turbulence flow involves two assumptions:

(a) the turbulence pattern is convected past the measuring point with the local mean speed;

(b) the turbulent fluctuating velocities are small enough compared to the mean motion to insure little change in the shape of an eddy as it is carried past a fixed point.

The use of this hypothesis in a shear flow has previously been questioned by Lin (1953). Essentially, Lin investigated the conditions for negligible eddy distortion and showed that there is 'no general justification of extending Taylor's hypothesis to the case of shear flow.' He found that unless an eddy component had a scale much less than the boundary-layer thickness, it would suffer significant distortion due to the mean-flow shearing motion while being carried past the measuring point by the mean flow. However, Lin's analysis did not lead to an alternative procedure for determining the turbulence scales.

We will show that, in general, assumption (a) cannot be valid in a turbulent shear flow. The departure from this assumption in a boundary layer is especially significant near the wall.

Consider a turbulent boundary layer on a flat plate. At any instant t, the turbulent fluctuation field in a boundary layer can be represented by a distribution of disturbance vorticity components ξ, η, and ζ throughout the boundary layer. At the wall the vertical perturbation velocity v must vanish. This boundary condition can be satisfied by adding an image vorticity distribution on the opposite side of the wall. Now, associated with the vorticity at a point P′ in the boundary layer, there is an induced velocity at the point P. The total velocity perturbation at point P at any instant can then be found by integrating over the boundary-layer and image-system perturbation vorticity fields. The extent of the region over which the integration must be carried out depends on the scale of turbulence. If only small-scale motions are present then the region of integration can be confined to the vicinity of P. There should not be any significant correlation between velocities at the point P and random small-scale vorticity at distances from P many times the scale of the disturbances. If large-scale motions are present then the integration must extend at least over the distances for which these large-scale motions are significantly correlated.

A typical one-dimensional energy spectrum for the velocity perturbation u in the flow direction at $y/\delta = 0{\cdot}58$ near the centre of a boundary layer is shown in figure 1, where y is the distance from the wall and δ is the boundary-layer thickness. If we can assume for the moment that this disturbance field is being carried along by the mean flow in accordance with Taylor's hypothesis, then the frequency can be converted into a measure of the space scale L by the relation $L = U_l/f$, where U_l is the velocity of the local mean flow (we will show that this is justified in the central region of the boundary layer).

Figure 1 also shows the contribution to the total energy $\overline{u^2}$ as a function of the scale of the motion. It is evident that fully half of the energy is contributed by

turbulence whose scale is more than twice the boundary-layer thickness, as first noted by Townsend (1951). Thus the velocity perturbation at a point P does not depend significantly on the vorticity in the immediate vicinity of P, but rather on the vorticity over an extensive region of the boundary layer.

Since the vorticity travels with the fluid particles, the apparent velocity with which a disturbance sweeps past the measuring point P may therefore be substantially different from the local mean velocity at P. For the large-scale motions, this disturbance velocity will correspond to the mean velocity near the middle of the boundary layer. Therefore for points P close to the wall, where the mean velocity is low, we would expect the disturbance velocity to be greater than the local mean velocity; for points P near the outer edge of the boundary layer, the disturbance velocity should be less than the local mean velocity.

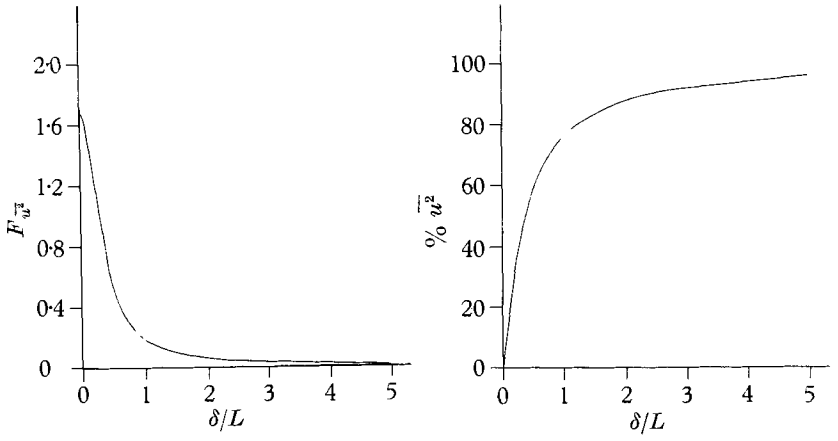

FIGURE 1. Typical boundary layer energy spectrum. $y/\delta = 0{\cdot}58$; from Klebanoff (normalized).

The space-time correlation data of Favre, Gaviglio & Dumas (1957, 1958) provide a basis for determining whether these deductions are correct. If $F(f)$ represents the percentage of turbulent energy associated with the frequency f, and Taylor's hypothesis is satisfied, then the auto-correlation coefficient R_x of the u' fluctuation at the points x_0 and (x_0+x), can be written as

$$R_x = \int_0^\infty F(f) \cos\left(\frac{2\pi x}{U_l} f\right) df,$$

where $R_x = \overline{u(x_0)\, u(x_0+x)}/\overline{u^2(x_0)}$, and x_0 represents the point P. The longitudinal correlation coefficient calculated in this way should then agree with the longitudinal correlation coefficient measured directly with two hot wires.

This auto-correlation coefficient has been calculated using the energy spectrum measured at one of Favre's test points and is shown in figure 2. The integration is only carried out to $f_{\max} = 1000$ c/s, but this includes 98% of the energy. In figure 2, two additional correlation curves are shown for which the integration was terminated at smaller values of the frequency, therefore eliminating the contribution of the small eddies. A frequency of 400 c/s corresponds to a longitudinal scale of about 2·4 cm which compares with a boundary-layer thickness of 3·4 cm.

It is evident that the correlation coefficient at large distances is not significantly affected by the small eddies. We shall confine our attention to the portion of the correlation curve determined by the large scale eddies so that R_x will be less than 0·4.

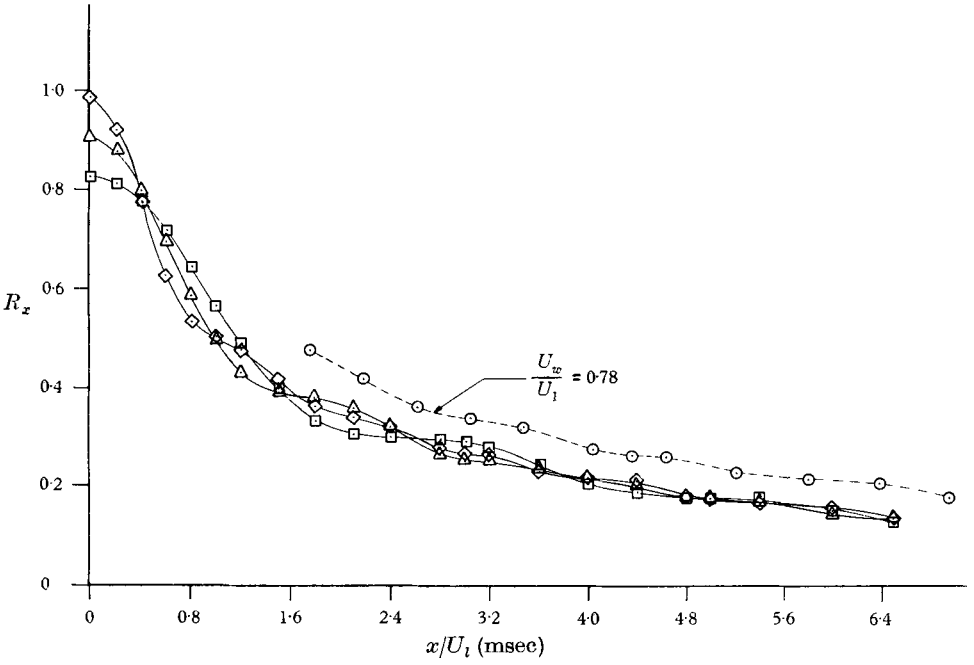

FIGURE 2. Effect of frequency cut-off and disturbance velocity on auto-correlation coefficient. Data from Favre *et al.*: $y/\delta = 0{\cdot}03$, $U_l/U_1 = 0{\cdot}54$; ◇, $f_{max} = 1000$; △, $f_{max} = 600$; ⊡, $f_{max} = 400$.

If the velocity of the disturbance U_w, associated with these large-scale eddies differs from the local mean velocity U_l, U_w rather than U_l must be used in the formula for computing the correlation coefficient from the energy spectrum at a fixed point. Thus, at a fixed value of R_x, the computed correlation curve should be shifted horizontally where the new horizontal co-ordinate $x' = xU_w/U_l$. Only the portion of the curve dominated by the large eddies should be shifted in this way, since as the eddy size is reduced, the disturbance velocity approaches the local mean velocity.

One of the figures from Favre's (1958) paper is reproduced in figure 3. Auto-correlation curves using Taylor's hypothesis and longitudinal space correlations measured with two hot wires are shown for four positions across a boundary layer. While there is the usual experimental scatter, there is a systematic difference between the two sets of curves below $R_x \approx 0{\cdot}4$ depending on the location of the measuring point in the boundary layer. Close to the wall the measured longitudinal correlation curves are to the right of the calculated auto-correlation curves. Near the outer edge of the boundary layer, the measured longitudinal correlation curve is displaced in the opposite direction. At $y/\delta = 0{\cdot}24$ the difference between the two curves is lost in the scatter of the data.

As far as they go, these measurements are consistent with the picture in which the large-scale disturbances which contain most of the energy move downstream at a mean velocity characteristic of the central region of the boundary-layer fluid. At $y/\delta = 0{\cdot}24$ in Favre's boundary layer, the velocity U_l is approximately equal to 0·78 of the free-stream velocity U_1. The horizontal shift in the correlation curve that would be expected at $y/\delta = 0{\cdot}03$ if the disturbance velocity were equal to $0{\cdot}78U_1$ is also shown in figure 2. This shift is approximately of the same

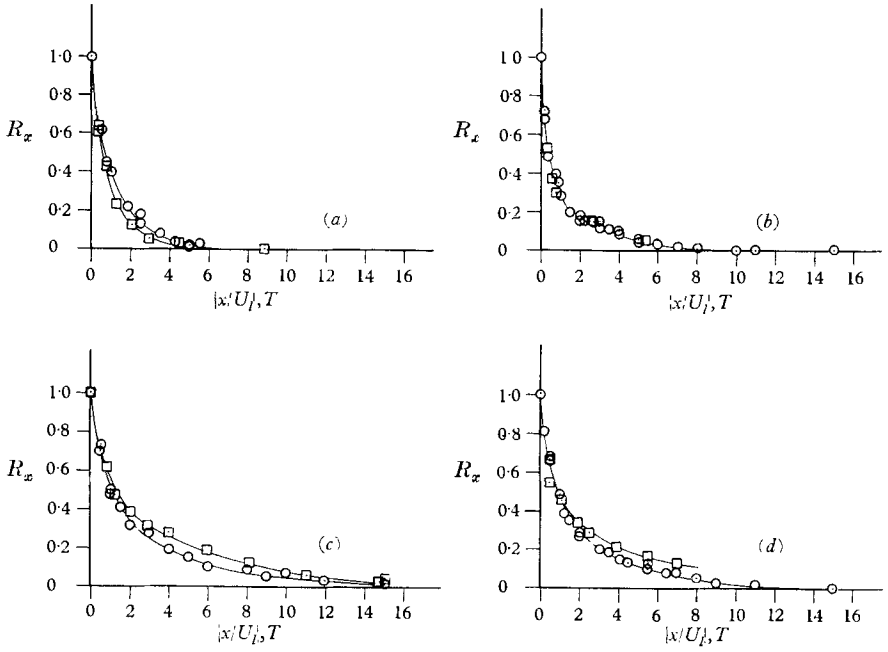

FIGURE 3. Comparison of auto-correlation and longitudinal correlation coefficients from Favre *et al.* ⊙, Auto-correlations; ⊡, longitudinal space correlations. (*a*) $y/\delta = 0{\cdot}77$, $R_\delta = 27{,}900$; (*b*) $y/\delta = 0{\cdot}24$, $R_\delta = 14{,}000$; (*c*) $y/\delta = 0{\cdot}15$, $R_\delta = 27{,}900$; (*d*) $y/\delta = 0{\cdot}03$, $R_\delta = 27{,}900$.

magnitude as the shift found in figure 3. A similar divergence of the calculated auto-correlation and measured longitudinal correlation coefficients at large scales has been observed by Klebanoff and led him to remark that 'this divergence gives rise to the interesting speculation that the large-scale motions have their own characteristic velocity different from the mean speed'.

We conclude, on the basis of this analysis, that in a boundary layer, or in fact, in any shear flow, the disturbance velocity at a point P is in general different from the local mean velocity. Therefore, the customary conversion of experimental spectral measurements into wave-numbers is invalid in a boundary layer anywhere near the wall except for the small-scale structure of the turbulence.

In the following sections of this paper, many of the numerical results will be based on the experimental measurements of Klebanoff. The limited auto-correlation and longitudinal correlation measurements he made do not extend to large enough scales to establish a value for the disturbance velocity of the large eddies with any precision. Accordingly, we shall use the general information

obtained from Favre's data and somewhat arbitrarily set $U_w = 0{\cdot}8U_1$ for the large eddies. This is the value of the mean velocity at $y/\delta = 0{\cdot}27$. We will also need to establish an approximate upper limit to the frequency range for which this disturbance velocity applies. Klebanoff's auto- and longitudinal correlation measurements indicate that for $R_x < 0{\cdot}5$, the expected shift of the longitudinal

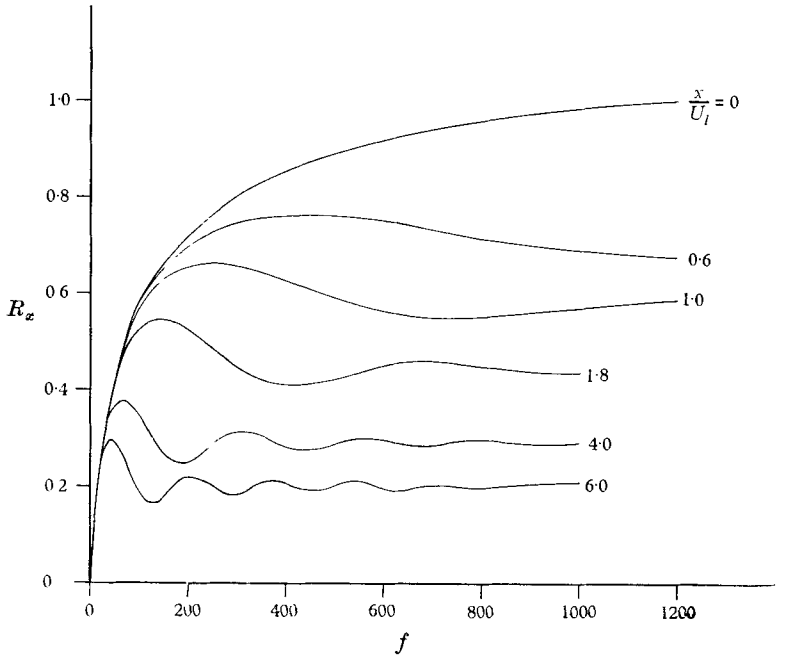

FIGURE 4. Auto-correlation functions for Klebanoff boundary-layer data.

correlation curve with respect to the auto-correlation curve will have occurred. Calculations for R_x as a function of frequency at different separations are shown in figure 4 for $y/\delta = 0{\cdot}05$. If we consider the curve for $x/U_l = 1{\cdot}8$, it is evident that the frequencies > 300 makes a minor contribution to the correlation coefficient, i.e. the frequencies between 300 and 1000 only produce a moderate oscillation about the final value of $R_x = 0{\cdot}43$. A frequency of 300 c/s corresponds to an eddy scale of $L = U_w/f \approx 4$ cm or approximately $\frac{1}{2}\delta$. (Frequencies in the range between $0 < f \leqslant 300$ c/s account for about 80 % of the fluctuation energy.) We will therefore limit the specification $U_w = 0{\cdot}8U_1$ to frequencies from 0 to 300 c/s. For high frequencies, or small-scale motions, the disturbances move downstream with the local mean velocity. A very crude guess for the dependence of disturbance velocity on frequency at $y/\delta = 0{\cdot}05$ will be given in the section on microscales. But Klebanoff's experimental data do not provide any clear basis for guessing at this dependence in the sublayer. As will be mentioned in the section on the pressure field, it may be possible to establish the variation of disturbance velocity with frequency for the higher frequencies from the measurements of wall pressure fluctuations. But at the present this information is not available and this lack of knowledge will necessarily limit certain possible applications of the present theory.

3. The fluctuation field across a turbulent flow

When the experimental measurements themselves are examined, they reveal a rather striking similarity of the energy spectra at different points in the fully turbulent part of the flow. The normalized energy spectra across a boundary layer as measured by Klebanoff are shown in figure 5. Over the inner half of the boundary layer, in the region free of intermittency, the spectra for the energy containing eddies appear to agree within the experimental error. Differences in

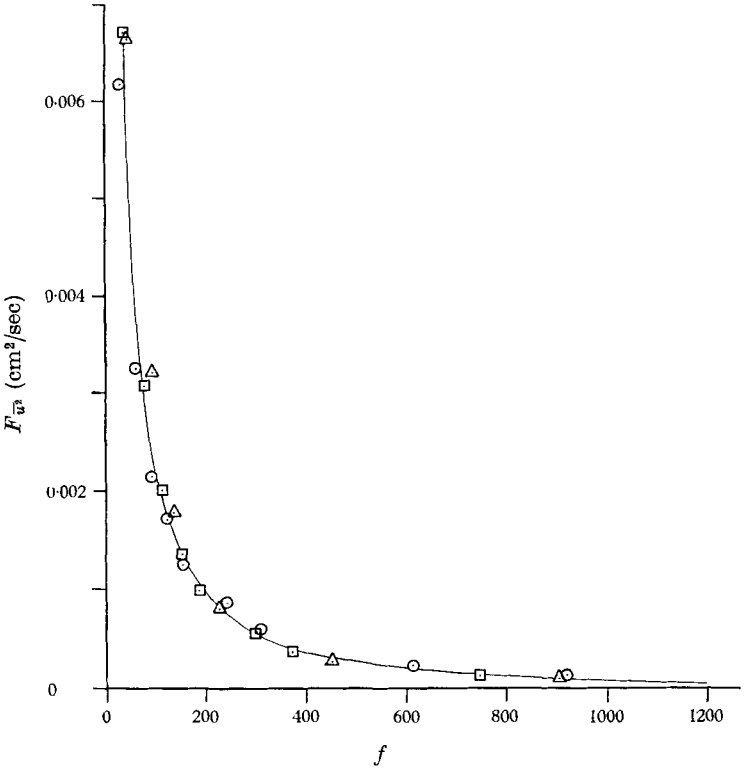

FIGURE 5. Normalized energy spectra at $y/\delta = 0{\cdot}05$ across boundary layer. ⊙, $Y/\delta = 0{\cdot}05$; ⊡, $Y/\delta = 0{\cdot}20$; △, $Y/\delta = 0{\cdot}58$.

the high-frequency end of the spectra would be revealed by using a logarithmic scale rather than a linear scale, but these portions of the spectra provide a negligible contribution to the total fluctuation energy. The same results are found for pipe- or channel-flow spectral data. This similarity of the energy-containing portion of the frequency spectra is just what would be expected from the previous analysis, since the disturbance velocity for the large-scale eddies should not vary significantly across the shear flow. At each point across the boundary layer, the hot-wire probe responds to disturbances associated with the same large-scale eddy pattern and so the spectral distribution should be similar. On the other hand, the fluctuation energy varies from point to point. Figure 6 shows the variation of the root-mean-square fluctuation velocities u', v' and w' across the

boundary layer. It can be seen that the u' fluctuation level increases by a factor of 2 between $y/\delta = 0{\cdot}6$ and $y/\delta = 0{\cdot}05$. Why does the fluctuation level vary if we are measuring perturbations due to the same large-scale eddy system?

A simple explanation for these observations can be suggested by considering the effect of the wall on the perturbation field. If no wall were present, the induced velocity field associated with vorticity at P′ would be symmetrical about P′. When the wall is present, the induced velocity field of the image vorticity for P′ must be added to the field directly due to P′. This will cause an increase in

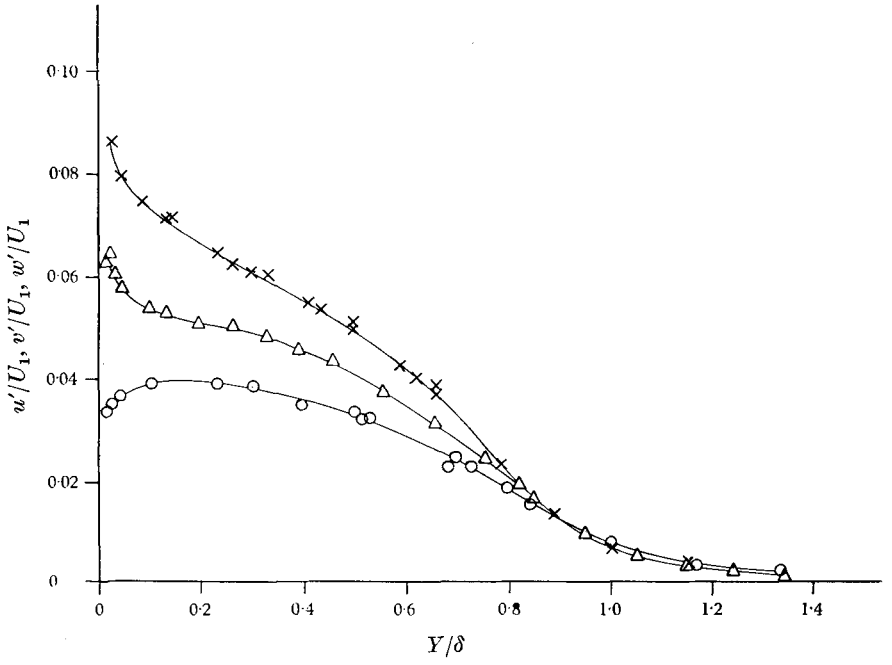

FIGURE 6. Variation of fluctuation levels across boundary layer. ×, u'/U_1; ○, v'/U_1; △, w'/U_1,

the induced velocities between P′ and the wall and a decrease in the induced velocities beyond P′. This image effect may be the reason why the fluctuation level associated with the same large-scale vorticity increases towards the wall.

So far we have managed to avoid specifying the extent of the sublayer. This has been a somewhat ambiguous question and has been subject to different interpretation by different authors. In figure 7, the variation of the u' fluctuation and the turbulent shear stress $\rho\overline{uv}$ near the wall are shown for a boundary layer and a pipe flow. The variation of $\rho\overline{uv}$ has been calculated using the measured mean velocity profile and the fact that the total shear stress is essentially constant near the wall. As is customary, the data are presented in terms of the friction velocity $U_\tau = (\tau_w/\rho)^{\frac{1}{2}}$, where τ_w is the friction at the wall and ρ is the density. We can describe what is observed in the following general terms. Outside the wall region, the turbulent shear stress and the u' fluctuation vary slowly compared to the variations that are found in the wall region. Entering the wall

region, the u' fluctuation first increases rising to a maximum well inside the wall region. At approximately the point where u' starts to rise, the shear stress starts to decrease slowly. The rapid decrease in u' is confined to the inner 25% of the wall region.

It would appear that the increase in fluctuation level in the wall region is greater for the boundary-layer flow. But this may not be true. With the existing

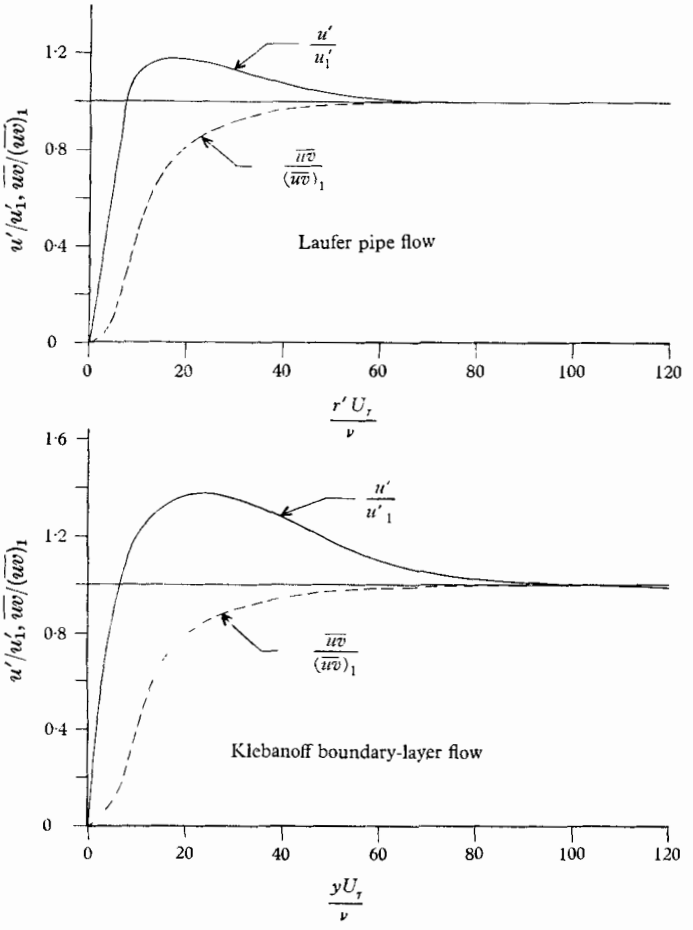

FIGURE 7. Fluctuation and turbulent shear stress near the wall from Klebanoff and Laufer.

data, it is not possible to pinpoint the edge of the wall region in the boundary-layer case because of the relatively large variation of u' outside the wall region. In figure 7, the fluctuation level is normalized in terms of the fluctuation level at the edge of the wall region and so the curve in figure 7 is somewhat arbitrary. Furthermore, the fluctuation level in the wall region should probably be compared with an extrapolation to the wall of the u' variation outside the wall region. This would reduce the apparent rise in fluctuation level for the boundary layer.

In the theory given in this paper, the sublayer and the wall region are the same so that the sublayer extends from the wall to the fully developed turbulent part

of the flow. There is no theoretical distinction between an inner 'laminar' sublayer and a transition region although the rapid changes do primarily occur in the inner portion of the sublayer.

The physical picture of the large-scale eddies containing most of the turbulent energy moving downstream at a velocity of the order of 0·8 of the free-stream velocity U_1 is reminiscent of the physical picture of oscillations in a laminar boundary layer. In that case typical waves move downstream with a velocity $U_w \approx \frac{1}{3}U_1$ and have wavelengths of the order of 2 to 5 δ. In the equations of motion for the perturbations in a laminar boundary layer, the term representing the action of viscosity is negligible except in two limited regions, the critical layer and the inner viscous layer close to the wall. We shall show that this inner viscous layer for fluctuations in a laminar boundary layer corresponds directly to the sublayer for a turbulent flow. Thus the sublayer is the region where the turbulent fluctuations in the shear flow are damped by viscosity.

The existence of a 'dissipation layer' near the wall was first suggested by Townsend on the basis of a study of the turbulent energy balance in the boundary layer. He concluded that the bulk of the turbulent-energy dissipation takes place by direct viscous action on the large eddies in a layer which he thought was 'most probably in contact with the laminar sublayer'. In the present theory we find that the sublayer itself is a dissipative region with its structure primarily determined by the large scale fluctuations in the turbulence.

4. Equations for the fluctuation field

The equations of motion for the fluctuations in a turbulent field (Lin 1959, p. 246) are obtained by subtracting the well-known Reynolds equation for the mean flow from the complete Navier–Stokes equations. We restrict our attention to a steady flow in which the mean velocity only has a component parallel to the flow direction, so that $U = U(y)$ and $V = W = 0$, where U, V and W are the three components of the mean motion. We will also assume that the statistical properties of the turbulent field such as $\overline{u^2}$ and $\overline{uv}$ only vary with y. These assumptions are reasonably well satisfied by a two-dimensional boundary-layer flow or a pipe flow. Then if u, v and w are the disturbance velocities the components of total velocity are $U+u$, v and w, and the pressure is $P+p$. We can then write down the three equations of motion for the fluctuating field,

$$\frac{\partial u}{\partial t}+U\frac{\partial u}{\partial x}+v\frac{\partial U}{\partial y}+u\frac{\partial u}{\partial y}+v\frac{\partial u}{\partial y}+w\frac{\partial u}{\partial z}=-\frac{1}{\rho}\frac{\partial p}{\partial x}+\nu\nabla^2 u+\frac{\partial}{\partial y}(\overline{uv}), \tag{1}$$

$$\frac{\partial v}{\partial t}+U\frac{\partial v}{\partial x}+u\frac{\partial v}{\partial x}+v\frac{\partial v}{\partial y}+w\frac{\partial v}{\partial z}=-\frac{1}{\rho}\frac{\partial p}{\partial y}+\nu\nabla^2 v+\frac{\partial}{\partial y}(\overline{v^2}), \tag{2}$$

$$\frac{\partial w}{\partial t}+U\frac{\partial w}{\partial x}+u\frac{\partial w}{\partial x}+v\frac{\partial w}{\partial y}+w\frac{\partial w}{\partial z}=-\frac{1}{\rho}\frac{\partial p}{\partial z}+\nu\nabla^2 w+\frac{\partial}{\partial y}(\overline{wv}) \tag{3}$$

and the continuity equation

$$\frac{\partial u}{\partial x}+\frac{\partial v}{\partial y}+\frac{\partial w}{\partial z}=0. \tag{4}$$

In each equation the mean term on the right is the average of the three non-linear terms on the left. We are in fact going to neglect these non-linear terms but some justification for this step is certainly required. For instance, the term $\partial(\overline{uv})/\partial y$ is zero at the wall and zero outside the sublayer, but reaches a peak value in the inner portion of the sublayer at about $U_\tau y/\nu \approx 10$ (see figure 7). We can make this justification *a posteriori* by finding a solution without the non-linear terms and then comparing the magnitude of $\partial(\overline{uv})/\partial y$ with the linear terms that have been retained. At this point we will state the results. The acceleration term $\partial u/\partial t$ is the leading linear term. At the point where $U_\tau y/\nu \approx 10$, $\partial(\overline{uv})/\partial y$ is about 15% of $[\overline{(\partial u/\partial t)^2}]^{\frac{1}{2}}$. At the same point the linear convective terms such as $U(\partial u/dx)$ are about 40% of $\partial u/\partial t$. It is evident that the non-linear terms are significant though smaller than the linear terms. When the balance of terms is examined over the frequency spectrum it is found that at the low end of the frequency spectrum, at say 10 c/s, the maximum value of $\partial(\overline{uv})/\partial y$ may be comparable in magnitude to the terms that are retained. But linearization of the equations appears to be a reasonable first step towards a theory. Of course the non-linear terms would be essential in any theory of turbulence. But here the turbulent field at the edge of the sublayer as well as the mean flow in the sublayer are assumed to be known from the experiments. Our purpose is merely to represent the fluctuation field between the known field at the edge of the sublayer and the wall.

The fluctuation field can now be represented by a superposition of Fourier components, each component of which can be separately analyzed. The type of disturbance that will be used will be based on our interpretation of the experimental data. It should be emphasized that we are not concerned with the energy balance of the frequency components as is the case for the study of oscillations in a laminar flow. No stability calculations are involved in the description of the sublayer.

5. Simplified theory

We have previously shown that most of the fluctuation energy near the wall is an induced field arising from vorticity distributed throughout the boundary layer. The type of elementary disturbance that is appropriate then depends on the nature of the large-scale vorticity in the boundary layer, and not on the vorticity field at the edge of the sublayer. Inasmuch as the root-mean-square w' fluctuation is approximately 0·7 of the root-mean-square u' fluctuation (figure 6), some type of 'three-dimensional' disturbance would appear to be necessary.

Physically, one might expect the shearing action of the mean flow to stretch out vortex lines in the direction of the mean flow. There might then be a preference in the large-scale motions for vortices nearly parallel rather than perpendicular to the wall. Since the induced velocities near the wall associated with a vortex line in the boundary layer are normal to the vortex line, the simple form of oblique disturbance at the edge of the sublayer shown in figure 8 would appear to be appropriate. In this elementary oblique disturbance, the lines perpendicular to the ξ-direction are lines of constant phase. The disturbance velocity q, in the (x, z)-plane, is in the ξ-direction and is periodic in space in the ξ-direction with a wavelength λ_ξ. The disturbance velocities u and w outside the sublayer are

then given by $u = q\cos\theta$, $w = q\sin\theta$, and the wavelength in the x-direction $\lambda_x = \lambda_\xi/\cos\theta$.

Actually, the form of elementary oblique disturbance that satisfies the complete linearized equations (1), (2) and (3) is more complicated than the disturbance shown in figure 8. The disturbance velocity q must also have a component normal to ξ to satisfy the equations of motion. However, in this section, we will develop a simplified theory in which the linear convective terms in equations (1), (2) and (3) are neglected. The form of disturbance shown in figure 8 does satisfy these simplified equations (5), (6) and (7) (see below).

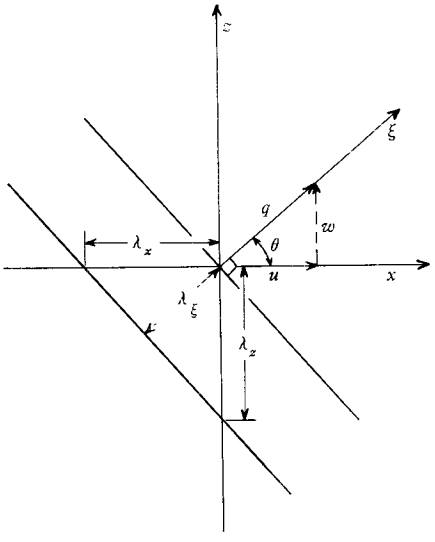

FIGURE 8. Assumed form of oblique disturbance at edge of sublayer.

As shown by the experimental data, the sublayer is very small and the scale of the energy containing eddies is large. Under these conditions, the variation of the perturbation velocity with y in the vicinity of the sublayer can be neglected compared to the variation inside the sublayer. The total fluctuation field can then be represented by a superposition of these elementary oblique disturbances.

This oblique disturbance is carried downstream with the velocity U_w in the x-direction. We now consider the disturbance velocities in the flow just outside the sublayer. Introducing complex notation, with $\beta = 2\pi f$ and $k_x = 2\pi/\lambda_x$, we have

$$u = \mathrm{Re}\{C_\theta \exp[i(k_x x + k_z z - \beta t)]\}, \quad w = \mathrm{Re}\{B_\theta \exp[i(k_x x + k_z z - \beta t)]\},$$

where $U_w = \beta/k_x$, $\tan\theta = B_\theta/C_\theta$, and Re stands for real part. Similarly, the fluctuating pressure field can be represented as

$$p = \mathrm{Re}\{p_\theta \exp[i(k_x x + k_z z - \beta t)]\},$$

where p_θ is complex.

Inside the sublayer, we have

$$u = \mathrm{Re}\{h(y) \exp[i(k_x x + k_z z - \beta t)]\}, \quad w = \mathrm{Re}\{k(y) \exp[i(k_x x + k_z z - \beta t)]\}.$$

There will also be a velocity component normal to the wall inside and outside the sublayer which we represent by

$$v = \mathrm{Re}\{g(y)\exp[i(k_x x + k_z z - \beta t)]\},$$

where the functions $h(y)$, $k(y)$, and $g(y)$ are complex. At the wall $y = 0$, $u = v = w = 0$.

Close to the wall where $u \to 0$ and $v \to 0$, some of the linear terms in equations (1), (2) and (3) can be neglected. The second term in each equation becomes small compared to the leading term. For instance, $\partial u/\partial x = ik_x u$, $\partial u/\partial t = -i\beta u$, so that

$$\left|U\frac{\partial u}{\partial x}\right| \Big/ \left|\frac{\partial u}{\partial t}\right| = \frac{U}{U_w}, \quad \text{which} \to 0 \quad \text{as} \quad y = 0.$$

Further, for all disturbances except those at large θ, the term $v\,dU/dy$ is also small compared to $\partial u/\partial t$ close to the wall. The vertical velocity can be found from the u- and w-components using the continuity equation $\partial v/\partial y = -\partial u/\partial x - \partial w/\partial z$, and the spatial derivatives given by

$$\partial u/\partial x = ik_x u, \quad \partial w/\partial z = ik_z w = ik_x w \tan\theta.$$

Then

$$v = \mathrm{Re}\left\{-\int_0^y ik_x u(y)\,dy - \int_0^y ik_x w(y)\tan\theta\,dy\right\}$$

or $v = O(\frac{1}{2}k_x uy\sec^2\theta)$ so that

$$\left|v\frac{\partial U}{\partial y}\right| \Big/ \left|\frac{\partial u}{\partial t}\right| = O\left(\frac{U}{2U_w}\sec^2\theta\right).$$

As we shall show later, the thickness of the viscous region for a disturbance of frequency f is

$$\delta_s = O\left(\sqrt{\frac{\nu}{f}}\right).$$

Then

$$\frac{\partial^2 u}{\partial x^2} \Big/ \frac{\partial^2 u}{\partial y^2} = O\left(\frac{4\pi^2 f\nu}{U_w^2}\right).$$

For any frequency of interest only the derivatives with respect to y need be retained. The equations of motion can then be simplified to the following form:

$$\frac{\partial u}{\partial t} + \frac{1}{\rho}\frac{\partial p}{\partial x} = \nu\frac{\partial^2 u}{\partial y^2}, \tag{5}$$

$$\frac{\partial v}{\partial t} + \frac{1}{\rho}\frac{\partial p}{\partial y} = \nu\frac{\partial^2 v}{\partial y^2}, \tag{6}$$

$$\frac{\partial w}{\partial t} + \frac{1}{\rho}\frac{\partial p}{\partial z} = \nu\frac{\partial^2 w}{\partial y^2}, \tag{7}$$

together with the continuity equation.

We cannot expect the solutions for the fluctuation field as given by these equations to be more than a first approximation. While the neglected convective terms are small very close to the wall, they are not small throughout the whole sublayer. By the edge of the inner part of the sublayer, at $y/\delta = 0{\cdot}008$, U/U_w has increased to 0·5. In addition, disturbances at high obliquity cannot be represented by equation (5) since the neglected term $v\,dU/dy$ would then become large. As

will be mentioned later, there are indications that disturbances with θ near 90° are important at the low-frequency end of the spectrum. In order to evaluate properly how much is left out by restricting the range of θ, we would like to know the orientation distribution of the energy containing eddies occupying the middle region of the boundary layer. Townsend (1956) has sought to determine eddy orientation in shear flows by comparing the transverse correlation functions. He concludes that in the main region of a turbulent boundary layer the larger eddies, containing perhaps 20 % of the turbulent energy, are strongly oriented in the flow direction. However, this method of analysis, in which possible eddy patterns are assumed, is rather speculative and it is not clear how much weight should be given to it. Nevertheless, Townsend's studies do suggest that large eddies near $\theta = 90°$ may play an important role in the fluctuation field.

On the other hand, the wave-numbers for the oblique disturbances which contribute to the total disturbance at the wave-number k_x are given by

$$k_\xi = k_x/\cos\theta, \quad \text{so that} \quad k_\xi \to \infty \quad \text{as} \quad \theta \to 90°.$$

Since the turbulent energy normally falls off very rapidly with increasing wave-number, there should be little contribution to the u fluctuation at a fixed k_x from disturbances with large θ. While this argument does not apply where $k_x \to 0$, it should apply to the wave numbers k_x containing most of the $\overline{u^2}$ energy.

It is evident that, to the order of simplification represented by equations (5), (6) and (7), there is no coupling between the u and w fluctuation fields and the u- and w-components can be solved for separately. In fact, $\overline{u^2}$ and $\overline{w^2}$ have the same variation with y in the viscous region. This is, of course, not true for solutions to the complete linearized form of equations (1), (2) and (3). In that case, the phase angle between the complex functions $h(y)$ and $k(y)$ varies with y, so that $\overline{u^2}$ and $\overline{w^2}$ for a disturbance vary differently with y in the viscous region.

An important feature of equations (5), (6) and (7) is that the pressure field is essentially invariant with y in the viscous region. We have

$$\frac{\partial}{\partial y}\left(\frac{1}{\rho}\frac{\partial p}{\partial x}\right) = \frac{ik_x}{\rho}\frac{\partial p}{\partial y}.$$

From equation (6),

$$\frac{1}{\rho}\frac{\partial p}{\partial y} = O\left(\frac{\partial v}{\partial t}\right).$$

Since $\partial v/\partial t = -i\beta v$,

$$\frac{\partial}{\partial y}\left(\frac{1}{\rho}\frac{\partial p}{\partial x}\right) = O\left(\tfrac{1}{2}k_x^2\beta uy\sec^2\theta\right)$$

or finally

$$\frac{\partial}{\partial y}\left(\frac{1}{\rho}\frac{\partial p}{\partial x}\right)\Big/\frac{\partial}{\partial y}\left(\frac{\partial u}{\partial t}\right) = O(\tfrac{1}{2}k_x^2y^2\sec^2\theta).$$

Similarly, it can be shown that

$$\frac{\partial}{\partial y}\left(\frac{1}{\rho}\frac{\partial p}{\partial z}\right)\Big/\frac{\partial}{\partial y}\left(\frac{\partial w}{\partial t}\right) = O\left(\tfrac{1}{2}k_x^2y^2\sec^2\theta\right).$$

Now at the edge of the viscous region, where $y = \delta_s$, $k_x\delta_s = O(2\pi\nu^{\frac{1}{2}}f^{\frac{1}{2}}/U_w)$. With $U_w = 1{\cdot}25 \times 10^3$ cm/sec, and $f = 300$ c/s, $k_x\delta_s = 3{\cdot}3 \times 10^{-2}$ or $k_x^2\delta_s^2 \ll 1$. In other words, in consequence of the fact that v is of higher order than q, the spatial pressure gradient associated with an oblique disturbance $\partial p/\partial\xi \ll \partial p/\partial y$ in the viscous region.

6. Longitudinal fluctuations

To find the solution to equation (5), we represent the disturbance as the sum of two components, where $u = u_1 + u_2$. The component u_1 represents the disturbance velocity before account is taken of the direct wall effect. As previously discussed, we assume that the variation of u_1 with y in the vicinity of the viscous region is negligible compared to the variation of u that occurs inside the viscous region. Since the convective terms have been neglected u_1 is not affected by the mean flow and is constant throughout the viscous region. u_2 represents the disturbance velocity component directly associated with the wall friction. Thus, at the edge of the viscous region $u_2 \to 0$, and at the wall $u_2 = -u_1$. If we write equation (5) as

$$\frac{\partial(u_1+u_2)}{\partial t} = -\frac{1}{\rho}\frac{\partial p}{\partial x} + \nu\frac{\partial^2(u_1+u_2)}{\partial y^2},$$

then the equations for u_1 and u_2 throughout the viscous region are

$$\frac{\partial u_1}{\partial t} + \frac{1}{\rho}\frac{\partial p}{\partial x} = O, \quad \frac{\partial u_2}{\partial t} = \nu\frac{\partial^2 u_2}{\partial y^2},$$

where, as we have already shown, $\rho^{-1}\partial p/\partial x$ does not vary through the viscous region.† Substituting $u_2 = h_2(y)\exp[i(k_x x - \beta t)]$, we have $h_2'' + \nu^{-1} i\beta h_2 = 0$, which which has the simple solution

$$h_2 = -\exp[-(1-i)(\beta/2\nu)^{\frac{1}{2}} y],$$

so that finally

$$u = u_1 + u_2 = \mathrm{Re}\{C_\theta(1 - \exp[-(1-i)(\beta/2\nu)^{\frac{1}{2}} y])\exp[i(k_x x - \beta t)]\}.$$

It is evident that the region of rapid change in u is $O(\nu^{\frac{1}{2}}/f^{\frac{1}{2}})$ as previously asserted so that the extent of the viscous region is different for each frequency, decreasing in size as the frequency is increased. In order to compare these results with experiment, we calculate $\overline{u^2} = \frac{1}{2}h(y)\,h^*(y)$, where the asterisk denotes the complex conjugate. Introducing the dimensionless variable $Y = (\beta/2\nu)^{\frac{1}{2}} y$, we find

$$\overline{u^2}/\tfrac{1}{2}C_1^2 = 1 - 2e^{-Y}\cos Y + e^{-2Y} \tag{8}$$

for the total disturbance energy. This function is shown in figure 9. For each frequency component, $\overline{u^2}/\frac{1}{2}C_1^2 \to 1$ at $Y \approx 5$. The rapid decrease of $\overline{u^2}$ occurs for $0 < Y < 2$. Entering the viscous region $\overline{u^2}/\frac{1}{2}C_1^2$ first increases reaching a peak value at $Y = 2{\cdot}2$. Examination of the details of the solution shows that this increase of disturbance level entering the viscous region arises because near the outer edge of the viscous region u_1 and u_2 have an in-phase component instead of being 180° out of phase as at the wall.

Figures 5 and 9 can now be used to calculate the variation of the root-mean-square fluctuation level u' near the wall. According to figure 5, the energy spectra are similar between $y/\delta = 0{\cdot}05$ and $y/\delta = 0{\cdot}58$. Then the disturbance energy for each frequency outside the viscous region is given by setting $\frac{1}{2}C_1^2 = F_{\overline{u^2}}$ at $y/\delta = 0{\cdot}05$ from figure 5. In the calculations, it has been assumed that C_1^2 is

† This same separation of equation (5) was used by Prandtl (1921) in discussing oscillations in a laminar boundary layer.

constant between the lowest frequency experimentally accessible and $f = 0$. Strictly speaking, $C_1^2 \to 0$ as $f \to 0$. According to the present theory, for very low frequencies, say $f < 1$ c/s, the point $y/\delta = 0{\cdot}05$ is in the inner portion of the viscous region (assuming that the simplified theory can be applied at such low frequencies), and the energy at $y/\delta = 0{\cdot}05$ should therefore $\to 0$ as $f \to 0$. However, the energy for $0 < f < 1$ c/s is negligible and makes no contribution to the calculations. Of course, without a wall present, the one-dimensional energy spectrum C_1^2 of a turbulent flow theoretically approaches a finite maximum as $f \to 0$.

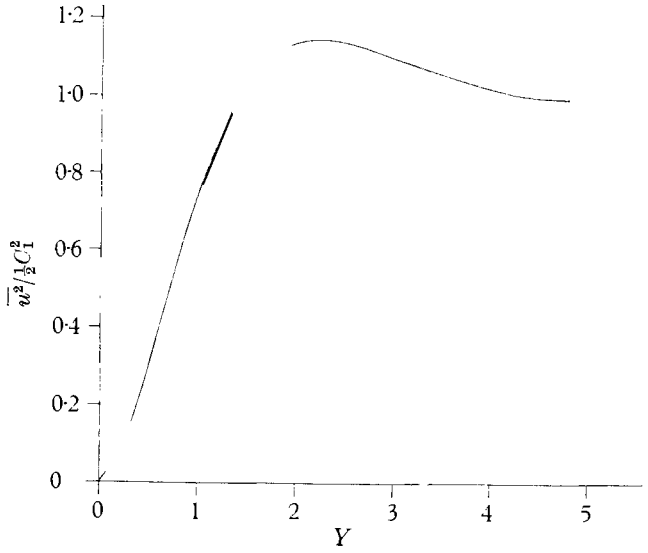

FIGURE 9. Theoretical variation of fluctuation energy in the viscous region.

For each frequency, the variation of $\overline{u^2}$ with y is obtained from figure 9. The $\overline{u^2}$ spectra for various values of y can then be computed and are shown in figure 10. As y/δ increases, the spectra approach the spectrum outside the sublayer. Integrating for each value of y/δ and taking the square root, we finally obtain the variation of u' near the wall. In figure 11*a*, the ordinate u'/u_1' is the ratio of u' inside the viscous region to the value of u_1' outside. According to the calculations, $u'/u_1' \to 1$ at about $y/\delta = 0{\cdot}035$. The rise in the experimental u' fluctuation level near the wall appears to start for $0{\cdot}03 < y/\delta < 0{\cdot}4$, but it is not possible to establish this point with any precision because of the variation of u' outside the sublayer. A comparison of Laufer's pipe data with similar theoretical calculations is shown in figure 11*b*. In both cases, the theory correctly predicts the total extent of the sublayer. On the basis of these calculations, we feel justified in identifying the viscous region in the theory with the sublayer in the experiments. On the other hand, the rise in fluctuation level entering the sublayer is much greater than the small rise found in the theory. Actually, the existence of an increase in fluctuation level in both theory and experiment is undoubtedly fortuitous. As mentioned previously, the rise in the theory depends on a delicate phase relationship which could hardly be expected to be unaffected by the neglected convective terms. By

$y/\delta = 0{\cdot}01$, the ratio U_l/U_w which is a measure of the relative magnitude of the convective terms is approximately 0·6, increasing to 0·75 by $y/\delta = 0{\cdot}035$. Thus, the agreement between theory and experiment should not be good in the outer region.

As shown in figure 10, there is a marked change in the spectral distribution approaching the wall. Most of the energy is taken from the largest-scale motions resulting in a fairly flat spectrum close to the wall. One spectral measurement was

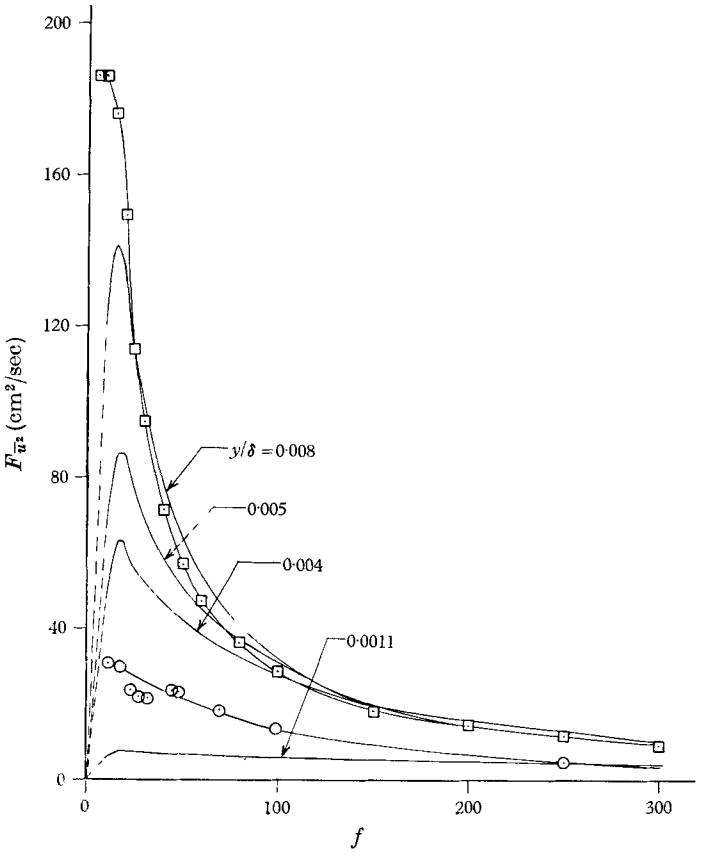

FIGURE 10. Energy spectra in the sublayer based on spectrum outside sublayer. Klebanoff spectra: ⊡, $y/\delta = 0{\cdot}05$; ⊙, $y/\delta = 0{\cdot}001$.

also made by Klebanoff at $y/\delta = 0{\cdot}0011$, deep in the sublayer. These measurements are also shown in figure 10 where they can be compared with the calculated spectrum for $y/\delta = 0{\cdot}0011$. Qualitatively, the measurements confirm the expectations of the theory. However, there is a significant difference in magnitude between theory and experiment at $y/\delta = 0{\cdot}0011$. A somewhat different way of applying the theory suggests itself.

Since we expect theory to be better near the wall, we can calculate the spectra in the sublayer based on the experimental spectrum at $y/\delta = 0{\cdot}0011$ rather than the spectrum outside the sublayer. Thus, using figure 9, the variation of $\frac{1}{2}C_1^2$ with f is chosen so that the theoretical and experimental spectra coincide at

$y/\delta = 0{\cdot}0011$. Then the corresponding spectra can be computed at other values of y/δ. The results are shown in figure 12 and the corresponding variation of u'/u_1' is shown in figure 11*a*. Here, of course, u'/u_1' for theory and experiment have been set equal at $y/\delta = 0{\cdot}0011$. The theoretical variation of u'/u_1' is now in much better

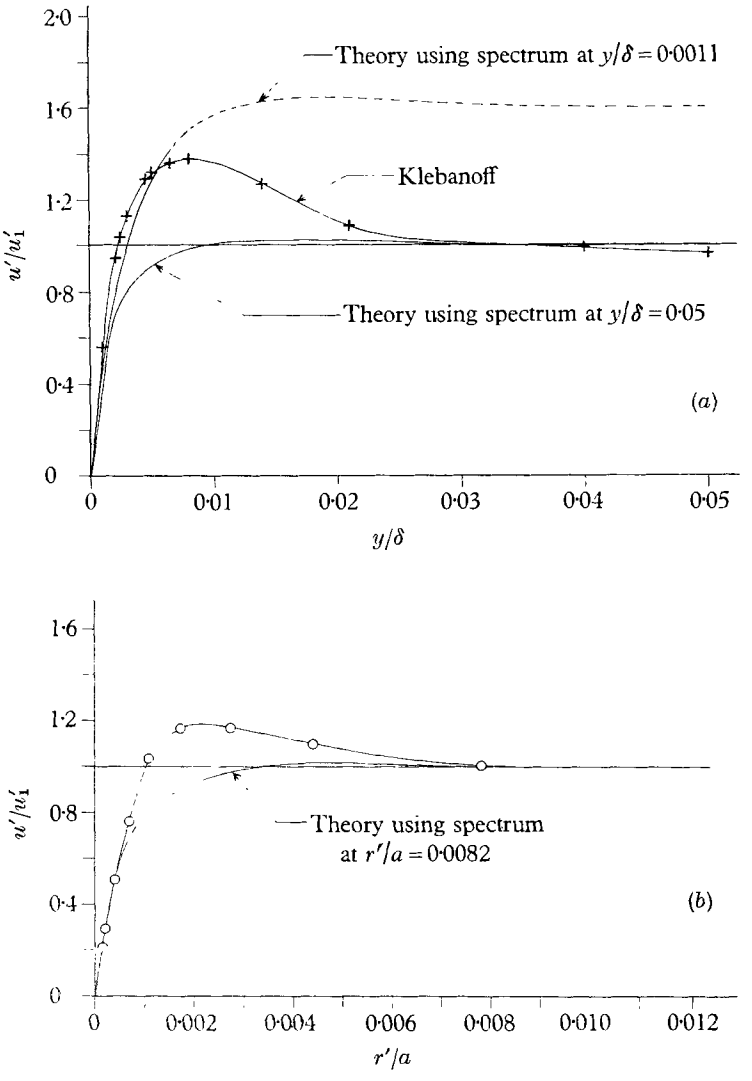

FIGURE 11. Comparison of theory and experiment for turbulent fluctuations in the sublayer: (*a*) boundary layer; (*b*) pipe flow, where a = pipe radius, R = 500,000; ⊙, data from Laufer.

accord with the experiments in the inner part of the sublayer, at least up to $y/\delta = 0{\cdot}005$ at which point $U/U_w \approx 0{\cdot}3$. Beyond $y/\delta = 0{\cdot}005$, the theoretical curve rapidly departs from the experimental data with the theory rising to a much higher value of u' outside the sublayer.

A comparison of the experimental spectrum at $y/\delta = 0{\cdot}05$ and the theoretical spectrum at $y/\delta = 0{\cdot}005$ (figure 12) indicates that the higher fluctuation level at $y/\delta = 0{\cdot}005$ is due to an increase in the energy in the large-scale eddies. This

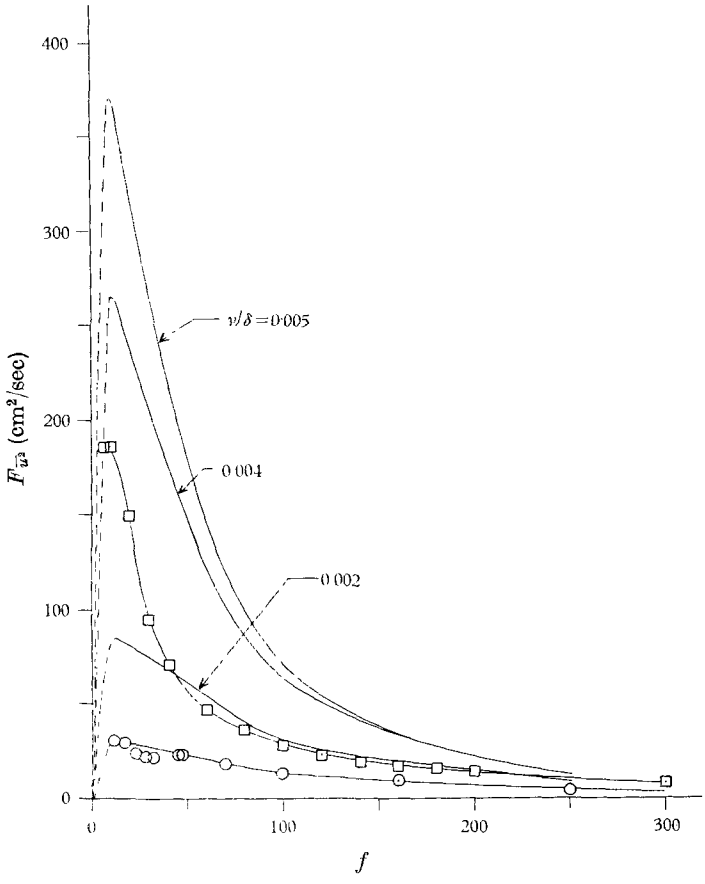

FIGURE 12. Energy spectra in the sublayer based on spectrum inside sublayer. Klebanoff spectra: ⊙, $y/\delta = 0{\cdot}0011$; ⊡, $y/\delta = 0{\cdot}05$.

is consistent with the theory in that at $y/\delta = 0{\cdot}005$, all frequencies above $f = 600$ c/s should still be outside the viscous region. Therefore, it seems probable that the spectra shown in figure 12 are a better representation of the spectra close to the wall than are the spectra in figure 10.

7. Transverse fluctuations and the shear stress

Expressions for $\overline{uv}$ and $\overline{v^2}$ for an oblique disturbance can also be obtained from the theory, but there are important difficulties in the way of using these expressions for comparison with the experiments. The limited comparisons that can be made indicate that the vertical velocity v and the shear stress $-\overline{uv}$ given by the theory may be much too small, at least at the low end of the frequency spectrum. Suppose we consider the disturbance velocities u_θ and v_θ associated with an oblique disturbance at angle θ, where $k_\xi = k_x/\cos\theta$. Since equations (5) and (7) are identical in form and $\rho^{-1}(\partial p/\partial z) = \rho^{-1}(\partial p/\partial x)\tan\theta$, the relation

$w_\theta = u_\theta \tan\theta$ holds throughout the viscous region. We can then readily find $\overline{v_\theta^2} = \frac{1}{2}g(y)\,g^*(y)$, so that

$$\overline{v_\theta^2} = (2\pi f\nu/U_w^2)\,\tfrac{1}{2}C_\theta^2\,(1+\tan^2\theta)^2\,T(Y), \tag{9}$$

where

$$T(Y) = \{(1-2e^{-Y}\cos Y + e^{-2Y}) + 2Ye^{-Y}(\cos Y - \sin Y) - 2Y + 2Y^2\}.$$

Here C_θ is the magnitude of u_θ at the edge of the viscous region.

Strictly speaking, the theory only gives the velocity field associated with a given disturbance in the viscous region for that frequency. It is not at all clear how far a simple disturbance can be followed outside the viscous region. This is important for the calculation of $\overline{v^2}$, since $\overline{v^2}$ for an elementary disturbance varies rapidly at the edge of the viscous region whereas $\overline{u^2}$ is essentially constant. With $\delta_s = O(\sqrt{\nu/f})$ this would automatically restrict calculations to very small y/δ. What this seems to mean is that the present theory is not capable of predicting the experimental results for $\overline{v^2}$ except possibly very close to the wall. It is also evident from equation (9) that there is a strong effect of the obliquity θ, and it would be necessary in any case to specify the energy distribution of oblique disturbances before it would be possible to compute $\overline{v^2}$ from the theory.

At the very low frequencies, the viscous region reaches out far enough to permit a comparison of sorts with the spectral measurements of $\overline{v^2}$ at $y/\delta = 0{\cdot}05$, since for $f = 10$ c/s the edge of the viscous region ($Y \approx 5$) is at $y/\delta \approx 0{\cdot}05$. If we consider a two-dimensional disturbance ($\theta = 0$), then it turns out that $\overline{v^2}$ at $f = 10$ c/s as given by equation (9) is too small roughly by a factor of 50. This suggests one of two things: either (*a*) the magnitude of $\partial u/\partial x$ given by the theory is much too small at the very low frequencies; overall, $\partial u/\partial x$ does appear to be the correct order of magnitude (see § 8); or (*b*) there is a substantial contribution to $\overline{v^2}$ at the very low frequencies from highly oblique disturbances; this would imply large vortices nearly aligned with the flow direction.

The computation of $\overline{uv}$ is beset by similar difficulties. According to the simplified theory, $(\overline{uv})_\theta = \frac{1}{2}\,\mathrm{Re}\{g(y)\,h^*(y)\}$ from which we obtain

$$(\overline{uv})_\theta = -\tfrac{1}{2}C_\theta^2(\pi f\nu)^{\frac{1}{2}}\,U_w^{-1}(1+\tan^2\theta)\,S(Y) \tag{10}$$

with $S(Y) = (1-2e^{-Y}\cos Y + e^{-2Y} - 2Ye^{-Y}\sin Y)$. The function $S(Y)$ is shown in figure 13 together with $(\overline{u^2}/\frac{1}{2}C_1^2)^{\frac{1}{2}}$.

It is evident that in the inner portion of the viscous region the relative variation of u' and $-\overline{uv}$ with y for each frequency component is similar to the over-all variation of u' and $-\overline{uv}$ shown in figure 7. Leaving the wall the increase in the shear stress lags behind the increase in the fluctuation level. In both experiment and theory, at the peak of the u' fluctuation $-\overline{uv}$ is 0·7 to 0·8 of the shear stress outside the viscous region. However, the magnitude of $-\overline{uv}$ given by the simplified theory is definitely too low over and above the fact that v may be too small This can be shown in the following way.

Sufficient data are given by Klebanoff to calculate the spectral variation of $\overline{uv}/u'v'$ at $y/\delta = 0{\cdot}05$. The results of the calculations are shown in figure 14. For comparison, the variation of $\overline{uv}/u'v'$ inside the viscous region according to the simplified theory is shown in figure 15. The correlation $\overline{uv}/u'v'$ is independent of θ

and a comparison with experiment shows whether the phase angles between u and v in the theory are at all comparable to the phase angles deduced from the experiment. Apparently the correlation coefficient does not reach high enough

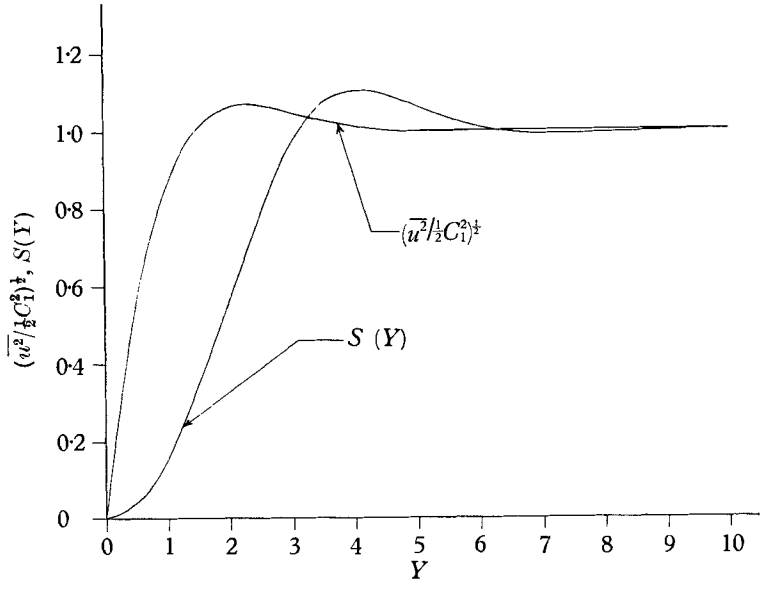

FIGURE 13. Theoretical variation of fluctuation level and turbulent shear stress in the viscous region.

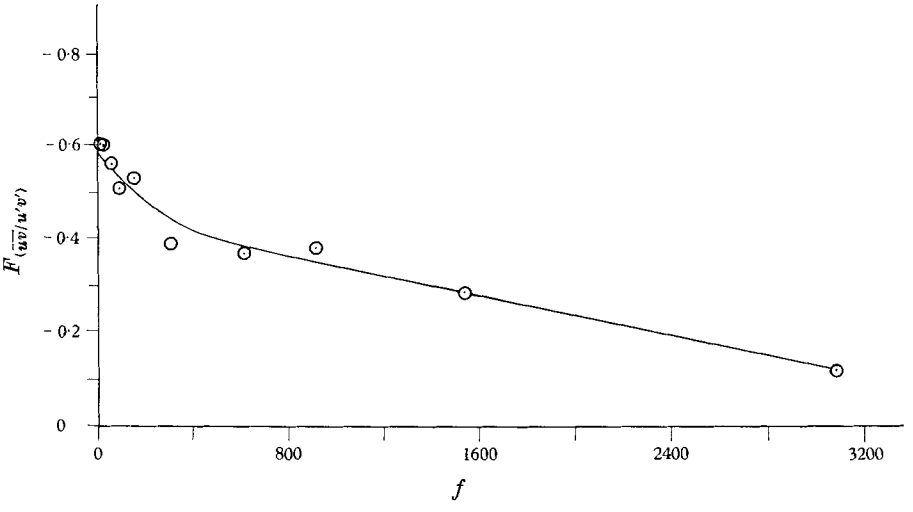

FIGURE 14. Variation of shear correlation coefficient with frequency outside sublayer after Klebanoff, ⊙, $y/\delta = 0{\cdot}05$.

values in the viscous region, at least at the lower frequencies. The convective terms that have been neglected in the simplified theory ought to play a significant role in controlling the phase angle between u and v. Therefore, this deficiency of the theory is not surprising.

Nevertheless, it is possible to draw some conclusions about the nature of the shear-stress spectrum in the sublayer, and so about the flow of energy from the mean flow to the fluctuating field. As shown by Reichardt (1953), the turbulence production $-\rho\overline{uv}(dU/dy)$ reaches a maximum in the sublayer at the point where $\mu(dU/dy) = \frac{1}{2}\tau_w$.

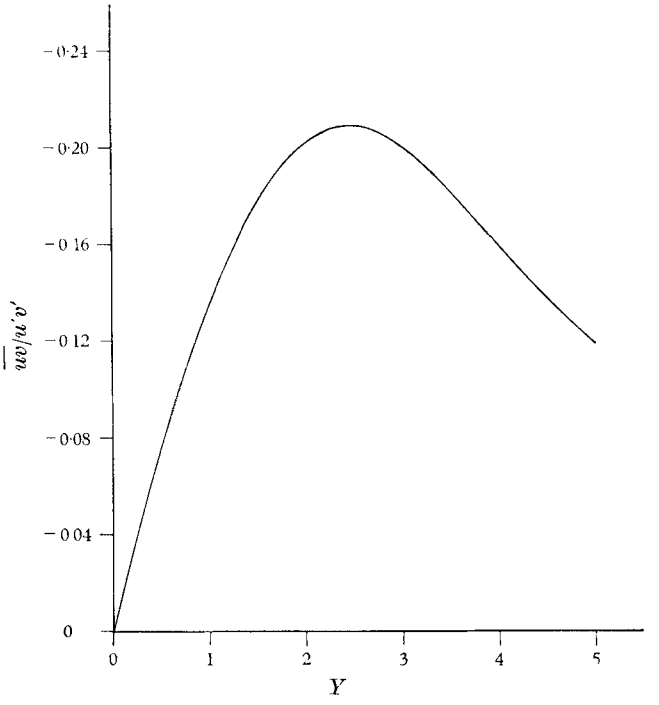

FIGURE 15. Theoretical variation of shear correlation coefficient in the viscous region.

Generally speaking, in the fully developed part of the boundary layer, the energy flows from the mean flow into the large-scale eddies. At $y/\delta = 0{\cdot}05$ from Klebanoff, 70 % of the shear stress is found between $0 < f < 300$, which compares with 80 % of $\overline{u^2}$ below $f = 300$. The point where $\mu(dU/dy) = \frac{1}{2}\tau_w$ is still outside the viscous region for the small eddies and the loss in turbulent shear stress comes only from the large-scale eddies. This means that the turbulence production goes into ever smaller eddies as the wall is approached as speculated by Klebanoff. Therefore the region of maximum turbulence production may be relatively unimportant as a source of energy for the large-scale energy-containing eddies in the boundary layer.

8. Microscales

Important changes in the dissipation derivatives or microscales occur on entering the sublayer. Here we will consider two of these derivatives which can be discussed, at least to a limited extent, using the simplified theory. The longitudinal microscale can be written as

$$\overline{(\partial u/\partial x)^2} = \tfrac{1}{2}k_x^2 \operatorname{Re}\{h(y)\,h^*(y)\} = (2\pi)^2 f^2 U_w^{-2}(\tfrac{1}{2}C_1^2). \tag{11}$$

While there are no data in general for the variation of the disturbance velocity U_w withf abovef = 300 c/s a first guess for this variation can be made at $y/\delta = 0.05$. For separation distances $\leqslant 0{\cdot}5$ cm, the auto-correlation and longitudinal-correlation curves of Klebanoff appear to coincide. This would suggest that $U_w = U_l$ where $f = U_l/0{\cdot}5$ cm or $f \approx 2 \times 10^3$ c/s. Previously, we have set an upper limit off = 300 c/s for $U_w = 0{\cdot}8U_1$. We assume then that the disturbance velocity

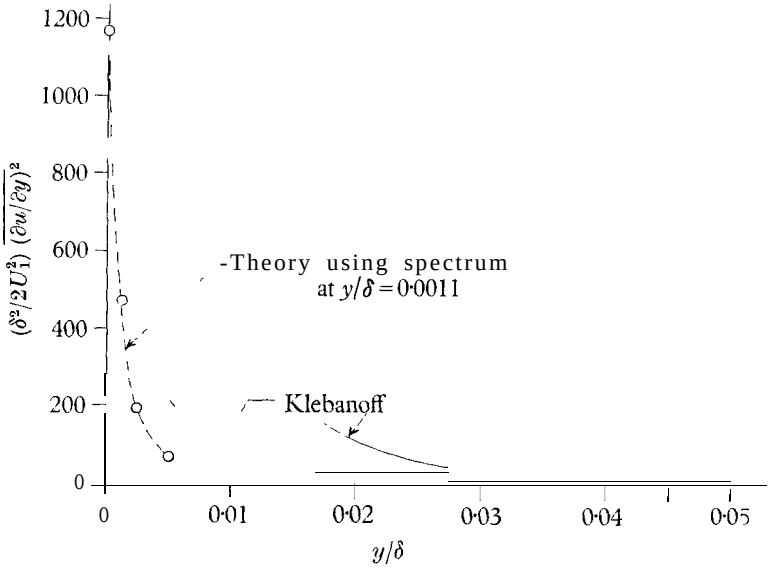

FIGURE 16. Comparison of theory and experiment for transverse microscale in the sublayer.

varies linearly from $0{\cdot}8U_1$ at $f = 300$ to $U_w = U_l$ at 2000 c/s. Above $f = 2000$ c/s, U_w is set equal to U_l. Integrating, we find that $(\delta^2/U_1^2)\,\overline{(\partial u/\partial x)^2} = 5{\cdot}8$ which compares with a value of 5·5 from the experiment. Deep in the sublayer the experimental value for $\overline{(\partial u/\partial x)^2}$ increases by about a factor of 3, but the uncertainty about the variation of U_w with f is too great to proceed with any theoretical calculations in this region.

The microscale transverse to the wall can be written as

$$\overline{(\partial u/\partial y)^2} = \tfrac{1}{2}h'(y)\,h'^*(y)$$

which becomes

$$\left(\frac{\partial u}{\partial y}\right)^2 = \frac{\pi f C_1^2}{\nu}\exp\{-2(\beta/2\nu)^{\frac{1}{2}}\,y). \tag{14}$$

Outside the sublayer, at y/S = 0·05, we have assumed a form of disturbance where $\partial u/\partial y = 0$, where in reality $\partial u/\partial y$ is small but not zero outside the viscous region. The experimental variation of $(\delta^2/2\,U_1^2)\,\overline{(\partial u/\partial y)^2}$ is shown in figure 16. Approaching the wall, there is a very rapid increase in the gradient normal to the wall. A rapid increase in $\overline{(\partial u/\partial y)^2}$ is also predicted by the theory. In fact, according to equation (12), $\overline{(\partial u/\partial y)^2}$ will be a maximum at the wall. Calculations have been carried out at several points in the inner part of the sublayer based on the

measured spectrum at $y/\delta = 0{\cdot}0011$, and the results are shown in figure 16. It is evident that the simplified theory underestimates the value of $\overline{(\partial u/\partial y)^2}$ at $y/\delta = 0{\cdot}005$, the inner limit of the experimental measurements. A possible reason for this discrepancy can be suggested. The large gradients in u in the simplified theory are confined to the region very close to the wall. Experimentally, as shown in figure 11, substantial gradients in u are found over a much greater extent of the sublayer. We might anticipate that the simplified theory would underestimate $\overline{(\partial u/\partial y)^2}$ away from the wall.

The much greater experimental value of $\overline{(\partial u/\partial y)^2}$ as compared with $\overline{(\partial u/\partial x)^2}$ does not reflect a distortion of the small-scale eddies. For instance at $y/\delta = 0{\cdot}005$, the theoretical spectrum for $\overline{(\partial u/\partial y)^2}$ shows that practically all the contribution to $\overline{(\partial u/\partial y)^2}$ comes from frequencies < 300 c/s.

9. The pressure field

Extensive measurements of the pressure fluctuations at the boundaries of turbulent flows have been made by Willmarth (1958, 1959). He found that the major contribution to the pressure fluctuations comes from large-scale fluctuations. Of particular interest, his space-time correlation measurements show that the pressure pattern is convected downstream with a speed of $0{\cdot}82U_1$. This observation is in good agreement with the present theory where the large-scale fluctuations move downstream at the mean velocity of the middle region of the boundary layer. In fact measurements of the wall pressure field may provide a means of establishing experimentally the variation of disturbance velocity with frequency for the higher frequencies in the sublayer. Corcos & Winkle (1960) have found that by making a spectral resolution of the longitudinal space-time correlation a functional relationship between convective velocity and frequency can be found. As we would expect theoretically the higher frequencies are convected more slowly than the low frequencies. However, theoretical calculation of the spectrum and the magnitude of the pressure fluctuations at the boundary layer is another matter.

The pressure fluctuations in a turbulent shear flow may be much larger than in a field of isotropic turbulence at comparable turbulent fluctuation levels. This is the case near the edge of the laminar sublayer in a turbulent boundary layer. Very large pressure fluctuations are associated with the linear terms in the equations of motion. Using the condition that the large eddies move downstream with $U_w \approx 0{\cdot}8U_1$, sufficient measurements of the fluctuation field have been made by Klebanoff to permit an approximate calculation of this pressure field. Just outside the sublayer, retaining all the linear terms, equation (1) becomes

$$\frac{\partial u}{\partial t} + U\frac{\partial u}{\partial x} + v\frac{\partial U}{\partial y} = -\frac{1}{\rho}\frac{\partial p}{\partial x}. \tag{13}$$

The fluctuation field at the edge of the sublayer is now represented by a superposition of Fourier components. Using the same notation as in the previous sections, we can write equation (13) as

$$p_1 = \rho U_w \left\{h(y)\left(1 - \frac{U_l}{U_w}\right)\frac{g(y)}{ik_x}\frac{d\,(U_l/U_w)}{dy}\right\}\exp\left[i(k_x x - \beta t)\right].$$

Then the spectral variation of $\overline{p^2}/\rho^2$ is given by

$$\frac{\overline{p^2}}{\rho^2} = (U_w - U_l)^2 F_{\overline{u^2}} + \frac{U_w^2}{(2\pi)^2 f^2}\left(\frac{dU_l}{dy}\right)^2 F_{\overline{v^2}} - \frac{U_w}{\pi f}(U_w - U_l)\frac{dU_l}{dy} F_{\overline{(iu)v}}. \tag{14}$$

In isotropic turbulence, $U_w = U_l$, $dU_l/dy = 0$, and the pressure field due to these linear terms vanishes. At high frequencies, $U_w = U_l$ and the first and third terms do not contribute to the pressure field. However, most of the contribution to the pressure fluctations comes from the moderate frequencies and these terms are important. The spectral functions $F_{\overline{u^2}}$ and $F_{\overline{v^2}}$ have been measured at the edge of the sublayer at $y/\delta = 0{\cdot}05$, and can be used directly in calculating $\overline{p^2}/\rho^2$. An additional assumption must be made in order to determine $F_{\overline{(iu)v}}$.

For a given frequency component, the shear correlation coefficient

$$\overline{uv}/u'v' = \cos\phi,$$

where ϕ is the phase angle between the u- and v-velocities. If we represent u on the positive real axis in the complex plane, then a negative correlation coefficient indicates that v is either in the second or third quadrants, since ϕ must lie between 90° and 270°. (According to the simplified theory, $180° < \phi < 270°$ throughout the viscous region, measuring ϕ counterclockwise from u.) Assuming then that v lies in the third quadrant, the correlation spectrum $F_{\overline{(iu)v}}$ can be computed using the variation of the experimental phase angle ϕ with frequency as given in figure 14. That is, if γ is the phase angle between iu and v, then $\cos\gamma = \sin\phi$, and $F_{\overline{(iu)v}}$ is negative making the third term in equation (14) positive. The resulting spectrum for $\overline{p^2}/\rho^2$ is shown in figure 17 where we have set $U_w = 0{\cdot}8U_1$. If v lies in the second instead of the third quadrant, then the sign of $F_{\overline{(iu)v}}$ is reversed although the magnitude is the same. In that case, the pressure-fluctuation spectrum would be represented by the lower boundary of the cross-hatched region in figure 17. The second term of equation (14), $(\overline{v^2}/k_x^2)\,(dU_l/dy)^2$, is also plotted in figure 17. It is evident that the principal contribution to the pressure field at the lower frequencies comes from this term. It follows that the simplified theory as given by equation (5) is completely inadequate for the determination of the pressure field at low frequencies, since in this equation the term $v\,dU/dy$ has been neglected.

It is interesting to compare these calculations with the pressure spectrum for an isotropic field, where the pressure fluctuations are due to the non-linear terms. Batchelor (1956, p. 181) has given an expression for the pressure fluctuations in an isotropic field in terms of the three-dimensional energy spectrum. The first step then is to find an appropriate energy spectrum for this flow. Since the Reynolds number of the turbulence is large, the one-dimensional spectrum $F_{\overline{u^2}}$ at $y/\delta = 0{\cdot}05$ can be fitted by the function

$$F_{\overline{u^2}} = \frac{L_x}{U_l}\left[\frac{4}{1 + (4\pi^2 f^2 L_x^2/U_l^2)}\right],$$

where L_x is the longitudinal integral scale (Dryden 1943). Then using the transformation between the one- and three-dimensional energy spectra for isotropic

turbulence, the three-dimensional spectrum $P(k)$ can be computed using Batchelor's theory where

$$\int_0^\infty P(k)\,dk = \overline{p^2}/\rho^2.$$

Finally, the one-dimensional pressure spectrum $F_{\tilde{p}}$, where we represent $\overline{p^2}/\rho^2$ by $\tilde{p}$, can be obtained from

$$F_{\tilde{p}} = \int_{k_x}^\infty \frac{P(k)}{k}\,dk$$

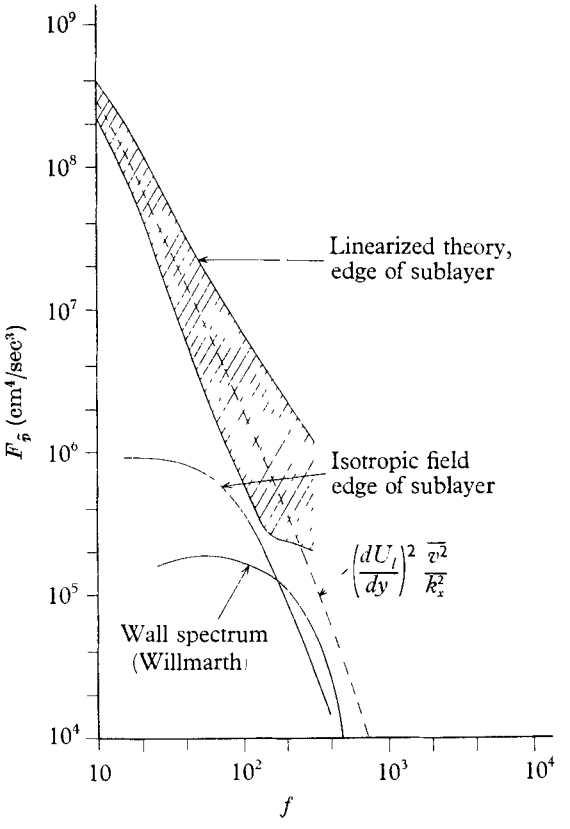

FIGURE 17. Pressure fluctuation spectra at edge of sublayer and at wall. $\tilde{p} = \overline{p^2}/\rho^2$.

and is also shown in figure 17 (transformed to a frequency spectrum). The values given are appropriate to an isotropic field with each component equal to u'. It is evident that at the edge of the sublayer, the linear terms are the main source of the pressure field.

The present theory provides a clear basis for having a pressure field at the boundary. For each frequency component $\partial(\partial p/\partial x)/\partial y \approx 0$ across the viscous layer. Even though the fluctuation components vanish at the wall, the pressure field does not vanish with them. This is in contrast to an isotropic pressure field, where $\overline{p^2}/\rho^2 \propto (u')^4$. One might then expect that at say $f = 10$ c/s, where the edge of the viscous region is at $y/\delta \approx 0{\cdot}05$, the pressure fluctuations at the boundary

would be of the same order as the pressure fluctuations at $y/\delta = 0{\cdot}05$. Using boundary-layer parameters appropriate to Klebanoff's experiment, Willmarth's wall measurements are also shown in figure 17. It is apparent that the wall pressure field is much smaller than what would be expected from the condition that $\partial(\partial p/\partial x)/\partial y \approx 0$. Integrating the spectra in figure 17, and taking the square root, we have $p'/\rho U_\tau^2 = 19$ to 30 for the linear terms, 3·7 for the isotropic field and 2·4 from Willmarth. Perhaps the non-linear terms that have been neglected are essential for the computation of the pressure fluctuations in the sublayer. A major contribution to the pressure field comes from the lowest frequencies and at these frequencies the non-linear terms are relatively more important. Or possibly the condition $\partial(\partial p/\partial x)/\partial y \approx 0$ may not be valid for the linear equations for highly oblique disturbances at low frequencies.

10. Laminar-turbulent transition in strong turbulence

The flow near the wall of a laminar boundary layer with strong free-stream turbulence is in many respects similar to the flow in the sublayer of a turbulent flow. The scale of the free-stream turbulence is in general large compared with the thickness of the laminar boundary layer. The free-stream turbulence moves downstream with the free-stream flow, and therefore at a disturbance velocity much larger than the local mean velocities in the boundary layer near the wall. In accordance with the present theory, we should expect to find a 'sublayer' of the free-stream turbulence in a small region close to the wall.

This suggests that the approach in this paper may be useful in dealing with the effect of free-stream turbulence on laminar boundary layers. Such a classical problem is the effect of strong free-stream turbulence on the Reynolds number of boundary-layer transition.

The most satisfactory correlation of the experimental data was given by Taylor (1936). Taylor derived his transition parameter on the assumption that the laminar boundary layer responds to the fluctuating pressure gradients of the turbulence in the same way that it would respond to a mean pressure gradient along the boundary. Taylor then assumed that if these fluctuating pressure gradients caused momentary separation of the laminar boundary layer, they would lead to transition.

There does not seem to be any theoretical basis for considering the turbulent pressure fluctuations as an exteral field acting on the laminar boundary layer. The turbulent fluctuations and their associated pressure gradients are inside the growing laminar boundary layer. The fluctuating field affects the mean flow through the shear stress not through the pressure fluctuations.

The present theory has been applied to the experimental conditions given by Dryden (1936), i.e. very strong free-stream turbulence. These data are at a transition Reynolds number based on the displacement thickness δ^* of $R_{\delta^*} \approx 500$, which appears to be the lowest transition Reynolds number to be found in the literature. This is very close to the minimum critical Reynolds number of $R_{\delta^*} = 400$ of the small disturbance stability curve for laminar boundary-layer oscillations. Accordingly, it should not be necessary to take into account the amplification of the disturbance level in the boundary layer in this case.

Liepmann, Laufer & Liepmann (1951) have measured the energy spectrum for the free-stream turbulence in a wind tunnel under experimental conditions reasonably close to those of Dryden. We estimate $L_x/U_1 \approx 1 \times 10^{-3}$ for Dryden, where $L_x/U_1 = 0{\cdot}9 \times 10^{-3}$ for Liepmann. Thus Liepmann's spectrum can be used to calculate the 'sublayer' for Dryden's experimental point. It is found that the disturbances due to the free-stream turbulence are damped down by viscosity in a 'sublayer' approximately 0·15 cm. thick. The close similarity between the physical picture for the sublayer of a turbulent flow and the 'sublayer' of the free-stream turbulence in a laminar boundary layer is shown in figure 18. The scale corresponding to 50 % of the $\overline{u^2}$ energy is shown in each diagram. It seems clear that the physical model used by Taylor, in which the mean boundary layer responds to the pressure gradients associated with the turbulence is not applicable to the description of the laminary boundary layer in strong free-stream turbulence.

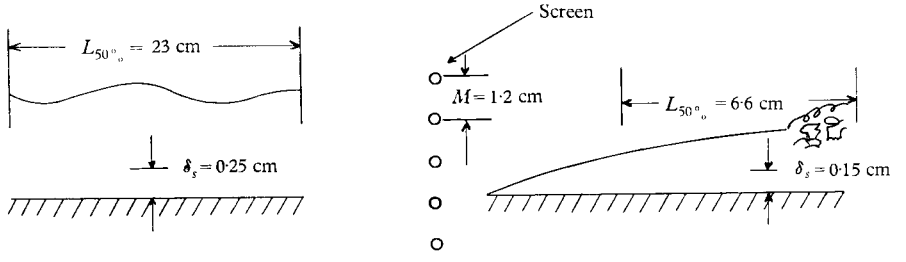

$U_1 = 1{\cdot}52 \times 10^3$ cm/sec
$\delta = 7{\cdot}6$ cm
$R_\delta = 7{\cdot}9 \times 10^4$
Turbulent boundary layer

$U_1 = 9{\cdot}9 \times 10^2$ cm/sec
$\delta_{tr} = 2{\cdot}28$ cm $u'/U_1 = 0{\cdot}03$
$R_{tr} = 1 \times 10^5$
Laminar—turbulent transition

FIGURE 18. Comparison of sublayers for boundary-layer turbulence and free-stream turbulence.

Nevertheless, Taylor's parameter does appear to correlate the available experimental data. We would now like to show that by introducing an additional physical assumption we can obtain a transition parameter very similar to that of Taylor's. No attempt will be made to justify this assumption here although it has led to reasonable results in some previous work (Lin, 1955, p. 90).

We assume that the onset of transition in very strong free-stream turbulence depends on the relative amplitude of the Reynolds stress associated with the turbulent fluctuations and the shear in the mean flow. That is, we adopt as a rough criterion for the onset of transition for this case the requirement that

$$-\rho\overline{uv} = f(R_{tr})\,\mu U/\delta.$$

From the simplified theory the shear stress outside the 'sublayer' is of the form $\rho\overline{uv} \propto \rho(u')^2 f^{\frac{1}{2}}\nu^{\frac{1}{2}}/U_w$. Here $U_w = U_1$, the free stream velocity. The frequency f can be replaced by $f = U_1/L_e$, where L_e represents the 'scale' of the turbulence. Then $-\rho\overline{uv} \propto \rho(u')^2\nu^{\frac{1}{2}}/(U_1 L_e)^{\frac{1}{2}}$. Now the thickness of the laminar boundary layer at transition is $\delta_{tr} \propto (x_{tr}\nu/U_1)^{\frac{1}{2}}$. Substituting, we have

$$\rho(u')^2\nu^{\frac{1}{2}}/(U_1 L_e)^{\frac{1}{2}} = f_1(R_{tr})\,\mu U_1^{\frac{3}{2}}/\sqrt{(\nu x_{tr})^{\frac{1}{2}}}.$$

Finally, we obtain

$$(u'/U_1)\,(x_{tr}/L_e)^{\frac{1}{4}} = f_1(R_{tr}).$$

Taylor's parameter is $$(u'/U_1)\,(x_{tr}/L_y)^{\frac{1}{5}} = f_2(R_{tr}),$$

where L_y is the lateral integral scale of the free-stream turbulence. The available transition data are too scattered to make it possible to distinguish between a $\frac{1}{4}$ or $\frac{1}{5}$ power variation with x_{tr}/L. From the point of view of correlating the experimental data, either parameter would be equally effective, although Taylor's parameter is based on the assumption that transition is caused by the small eddies, whereas for the new parameter it is assumed that transition is caused by the large eddies.

11. Concluding remarks

The vorticity field responsible for the turbulent fluctuations in a boundary layer or similar shear flow is swept along with the velocity of the fluid elements. The velocity fluctuation field associated with this vorticity field is altered by the wall in two ways. The effect of the boundary condition $v = 0$ is to increase the magnitude of the wall velocity fluctuations u and w in the plane of the wall. The induced velocity at the wall associated with each element of vorticity is doubled by the image vortex element required to cancel v at the wall. This form of 'wall effect' extends across the boundary layer and beyond into the potential flow. As a result of the boundary conditions $u = w = 0$ the turbulent velocity fluctuations are directly damped down by viscosity in a thin layer, the sublayer.

The equations of motion for the turbulent velocity and pressure fluctuations are applied only in this narrow viscous region. The aim of the theory is to say, in detail, how a known turbulent field is damped by the wall. A simplified form of the theory is given in this paper. Only the leading terms in the differential equations are retained. Furthermore, while the three-dimensional character of the fluctuation field is recognized and introduced at any early stage, the calculations are not carried far enough to make the three-dimensionality important.

The same basic approach can be used to develop a more accurate description of the sublayer. The linear convective terms can be retained in the equations and solutions obtained using computing machines. When the convective terms are retained, disturbances at any obliquity can be considered.

Ordinarily, a distinction is made between a laminar sublayer, where the mean velocity profile is linear, and a 'transition' zone between this laminar sublayer and the fully turbulent part of the flow. No such distinction is made in this paper. The viscous sublayer is the entire region between the wall and the fully turbulent part of the flow.

Finally, there are related problems in which the present approach may be useful. We have already shown that the theory applies to the 'sublayer' of the free-stream turbulence in a laminar boundary layer. A similar approach might be useful in the description of turbulent heat and mass transfer.

REFERENCES

BATCHELOR, G. K. 1956 *The theory of Homogeneous Turbulence*, p. 181. Cambridge University Press.

CORCOS, G. M. & VON WINKLE, W. 1960 Measurements of the pressure field at the boundary of a fully developed turbulent pipe flow. *Bull. Amer. Phys. Soc.* Series II, **5**.

DRYDEN, H. L. 1936 Air flow in the boundary layer near a plate. *NACA Rep.* no. 562.

DRYDEN, H. L. 1943 A review of the statistical theory of turbulence. *Quart. Appl. Math.* **1**, 7.

EINSTEIN, H. A. & LI, H. 1956 The viscous sublayer along a smooth boundary. *Proc. Amer. Soc. Civ. Engrs.* Paper 945.

FAGE, A. & TOWNEND, H. C. H. 1932 An examination of turbulent flow with an ultramicroscope. *Proc. Roy. Soc.* A, **135**, 656.

FAVRE, A. J., GAVIGLIO, J. J. & DUMAS, R. J. 1957 Space-time double correlations and spectra in a turbulent boundary layer. *J. Fluid Mech.* **2**, 313.

FAVRE, A. J., GAVIGLIO, J. J. & DUMAS, R. J. 1958 Further space-time correlations of velocity in a turbulent boundary layer. *J. Fluid Mech.* **3**, 344.

HANRATTY, T. J. 1956 Turbulent exchange of mass and momentum with a boundary. *Amer. Inst. Chem. Engrs.*, **2**, 359.

KLEBANOFF, P. S. 1954 Characteristics of turbulence in a boundary layer with zero pressure gradients. *NACA Tech. Note* no. 3178.

LAUFER, J. 1950 Investigations of turbulent flow in a two-dimensional channel. *NACA Tech. Note* no. 2123.

LAUFER, J. 1953 The structure of turbulence in fully developed pipe flow. *NACA Tech. Note* no. 2954.

LIEPMANN, H. W., LAUFER, J. & LIEPMANN, KATE 1951 On the spectrum of isotropic turbulence. *NACA Tech. Note* no. 2473.

LIN, C. C. 1953 On Taylor's hypothesis and the acceleration terms in the Navier–Stokes equations. *Quart. Appl. Math.* **10**, 295.

LIN, C. C. 1955 *The Theory of hydrodynamic Stability*. Cambridge University Press.

LIN, C. C. 1959 (editor) *High Speed aerodynamics*, vol. v, p. 246. Princeton University Press.

PRANDTL, L. 1921 Bemerkungen über die entstehung der turbulenz. *Z. angew. Math. Mech.* **1**, 431.

REICHARDT, H. 1953 Die Energieversorgung der Wandturbulenz. *Z. angew. Math. Mech.* **33**, 336.

TAYLOR, G. I. 1916 Conditions at the surface of a hot body exposed to the wind. *Brit. Adv. Comm. Aero. Rep. & Mem.* no. 272.

TAYLOR, G. I. 1932 Note on the distribution of turbulent velocities in a fluid near a solid wall. *Proc. Roy. Soc.* A, **135**, 678.

TAYLOR, G. I. 1936 Statistical theory of turbulence, Part V. *Proc. Roy. Soc.* A, **156**, 307.

TAYLOR, G. I. 1938 The spectrum of turbulence. *Proc. Roy. Soc.* A, **164**, 476.

TOWNSEND, A. A. 1951 The structure of the turbulent boundary layer. *Proc. Camb. Phil. Soc.* **47**, 375.

TOWNSEND, A. A. 1956 *The Structure of turbulent Shear Flow*, p. 249. Cambridge University Press.

WILLMARTH, W. W. 1958 Wall pressure fluctuations in a turbulent boundary layer. *NACA Tech. Note* no. 4139.

WILLMARTH, W. W. 1959 Space-time correlations and spectra of wall pressure in a turbulent boundary layer. *NASA Memo*, no. 3-17-59W.